Neutron Diffraction Study of *Pseudomonas aeruginosa* Lipopolysaccharide Bilayers

Thomas Abraham,[*,†,‡] **Sarah R. Schooling,**[‡,§] **Mu-Ping Nieh,**[†] **Norbert Kučerka,**[†]
Terry J. Beveridge,[‡,§,∥] **and John Katsaras**[*,†,‡,∥,⊥]

*National Research Council, Canadian Neutron Beam Center, Chalk River, Ontario K0J 1J0, Canada,
Department of Molecular and Cellular Biology University of Guelph, Ontario N1G 2W1, Canada,
Biophysics Interdepartmental Group and Guelph-Waterloo Physics Institute, University of Guelph, Guelph,
Ontario N1G 2W1, Canada, Advanced Food and Materials Network—Networks of Centers of Excellence,
Guelph, Ontario N1G 2W1, Canada, and Department of Physics, Brock University, 500 Glenridge Avenue, St.
Catharines, Ontario L2S 3A1, Canada*

Received: September 14, 2006; In Final Form: December 5, 2006

Lipopolysaccharides (LPSs) are a major class of macromolecules populating the surface of Gram-negative bacteria. They contribute significantly to the bacterium's surface properties and play a crucial role in regulating the permeability of its outer membrane. Here, we report on neutron diffraction studies performed on aligned, self-assembled bilayers of LPS isolated from *Pseudomonas aeruginosa* PAO1. This LPS system is comprised of a mixture of rough and smooth A-band and B-band LPS, similar to that naturally found in *P. aeruginosa*. Temperature scans were conducted at various levels of hydration, and the phases adopted by LPS, along with their corresponding transition temperatures, have been identified. Because of LPS's chemical heterogeneity, the gel-to-liquid-crystalline transition was continuous and not abrupt as commonly observed in single-component phospholipid systems. From the construction of one-dimensional scattering length density profiles, we find that water penetrates into the hydrocarbon region up to and including the center of liquid-crystalline LPS bilayers. This permeability to water also extends to bilayers in the continuous phase transition region and could have far-reaching implications as to how small molecules penetrate the outer membrane of Gram-negative bacteria.

Introduction

Lipopolysaccharide (LPS) is an essential macromolecular component of the outer membrane (OM) of Gram-negative bacteria[1−3] and arranges itself in such a manner that it is found almost exclusively on the outer face of the OM.[4,5] Here, five to six 2- or 3-hydroxyl fatty acid acyl chains extend from a phosphorylated diglucosamine backbone cementing the macromolecule into the hydrophobic domain of the bilayer.[1−3] A charged core oligosaccharide extends above the diglucosamine backbone to which an O-side chain of repeating sugars is often attached. In *Pseudomonas aeruginosa*, this O-side chain can be highly variable in composition and length.[2] In terms of mass, LPS accounts for ∼50% of the OM with other bacterial phospholipids and proteins making up the remainder.[6]

P. aeruginosa is an opportunistic pathogen that has been implicated in a number of difficult-to-treat diseases including, burn-patient and necrotic eye infections as well as chronic lung disease in cystic fibrosis patients.[2] It is a major cause of nosocomial infection and especially difficult to treat through conventional antibiotic therapy. Its resistance to antibiotics is sometimes related to surface antibiotic exclusion and LPS chemotype. The major LPS species produced by strain PAO1

is the pentaacyl form,[7] although the degree of acylation is highly dependent on both the strain of bacteria and its environmental conditions.[7,8] As mentioned, the acyl chains embed the LPS in the membrane with the diglucosamine covalently bound to the inner core region. The inner core oligosaccharide consists of two 2-keto-3-deoxyoctonate (KDO) molecules and two heptose molecules bearing phosphoryl groups. The chemistry of the outer core region, however, is more variable and also depends on whether the core bears an O-side chain or not.[9,10] In *P. aeruginosa*, the O-side chain may consist of one of two chemotypes termed A-band (common antigen, found on all except rough strains) or B-band (O-specific antigen, the basis for serotyping).[2] The A-band chain is a neutral homopolymer of D-rhamnose, while B-band LPS carries a net negative charge and consists of a linear polymer of di- to pentasaccharide repeat units. In PAO1, the B-band is composed of trisaccharide repeats of 2-acetamido-3-acetamidino-2,3-dideoxymannuronic acid, 2,3-acetamido-D-mannuronic acid, and *N*-acetylfucosamine.[2,7]

It is well-established that LPS plays a crucial role in the structure and integrity of the OM as well as controlling the permeability of various molecules, including nutrients and antimicrobials.[1] It should also be mentioned, however, that outer membrane proteins (OMPs) such as porin, which assemble into membrane-spanning multimeric channel complexes, also have an important bearing on membrane permeability.[1] Additionally, by virtue of being located at the cell surface, LPS contributes to the cell's overall surface properties with implications for various chemical interactions with the cell.[1,2] Indeed, some surface properties are easily observable, as in the case of cells with O-side chains attached to the core oligosaccharide, which

---

* To whom correspondence should be addressed. E-mail: Thomas.Abraham@nrc.gc.ca (T.A.); John.Katsaras@nrc.ca (J.K.).
† Canadian Neutron Beam Center.
‡ Advanced Foods and Materials Network—Networks of Centers of Excellence.
§ Department of Molecular and Cellular Biology, University of Guelph.
∥ Biophysics Interdepartmental Group and Guelph-Waterloo Physics Institute, University of Guelph.
⊥ Brock University.

form smooth shiny colonies on a solid growth medium. This type of LPS is termed smooth- or S-LPS, whereas LPS without the O-side chain is termed rough- or R-LPS.

There have been many studies on LPS to establish its location in the OM[4,5] and determine its interactions with itself and with OMPs, its dependence on natural metal cations for integrity, and the way it is perturbed by surface active antimicrobials, detergents, and organic solvents.[1,11] However, its solvation properties have not been studied extensively, as there are few techniques which can accurately monitor the macromolecule's solvation by water, even though solvation may extensively affect the properties of the OM. As a result, we chose to study the solvation properties of self-assembled LPS bilayers using neutron scattering, a technique particularly sensitive to water and its location within the bilayer. As mentioned, the extent of hydration may have a direct impact on the properties of the OM and the information provided by neutron scattering may help us better understand bacterial interactions, such as host−parasite interactions and resistance to hydrophobic antibiotics and antimicrobial peptides.

X-ray diffraction studies performed on partially hydrated LPS and lipid A films,[12−14] osmotically stressed self-assembled multibilayers,[15] and LPS dispersions[16] have shown that isolated LPS forms symmetric bilayers. In addition, Snyder et al.[15] and Garidel et al.[16] have emphasized the importance of cations in particular, multivalent cations in the formation of water impermeable LPS bilayers. X-ray diffraction studies using fully hydrated suspensions have also shown that LPS can adopt a number of morphologies including, under certain pH and ionic strength conditions, non-lamellar structures.[17,18] To obtain finer organizational and structural detail, Snyder et al.[15] and Ding et al.[14] carried out X-ray diffraction studies whereby they varied the hydration levels of LPS multibilayers, thus determining the phase component of the structure factor, while others have used less rigorous methods in obtaining this phase information.[13,16] Despite these reports, many of which utilized R-LPS or lipid A, structural studies of natural LPS systems containing S-LPS are to date lacking. This is striking especially when one considers the relative abundance of available information pertaining to phospholipid systems.[19,20] One of the main reasons for this paucity of LPS structural information is the difficulty in manipulating this heterogeneous system. Additionally, the manufacturing of aligned LPS multibilayer stacks necessary for good quality diffraction measurements is not trivial. However, given the known importance and prevalence of the O-side chain in LPS, it is worthwhile to elucidate the structural details of an LPS system which better approximates the native biological system.

There are a number of open questions regarding the phase and corresponding permeabilities of LPS. To date, there are no reports using neutron diffraction to study self-assembled LPS bilayers despite the ability of neutrons to differentiate between the various LPS chemical moieties and more importantly, their unique ability to distinguish between hydrogen and deuterium. As an outcome of the latter, determining the sign of the structure factor is made possible simply by varying, in a systematic manner, the H_2O/D_2O ratio. From there, it is relatively straightforward to reconstruct the one-dimensional scattering length density (1D SLD) profile, which besides resolving the structural detail of the LPS bilayer also determines the location of water.

Here, we report on neutron diffraction studies carried out using LPS isolated from *P. aeruginosa* PAO1 (serotype O5). Temperature scans were conducted at various levels of hydration
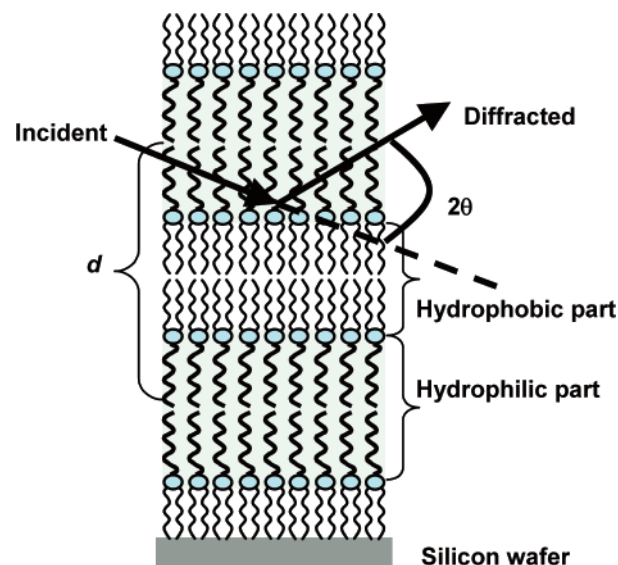

Figure 1. Schematic of oriented LPS multibilayers on a silicon substrate. The legend *d* denotes the *d*-spacing or the inter-lamellar spacing. See text for details.

and the transition temperatures identified. The morphology, transition temperature, and lamellar repeat spacing (*d*-spacing) were found to be influenced by the level of hydration. In order to better characterize the structural details of these bilayers and to specifically address the issue of water permeability, the higher-order Bragg peaks of liquid-crystalline (L_α) LPS bilayers as well as those in the continuous transition region were collected. From these measurements, we were able to construct the 1D SLD profile as a function of temperature and phase. The central finding is that L_α bilayers formed from LPS isolated from *P. aeruginosa* are highly permeable to water, and this result extends to those same bilayers in the continuous transition regime.

Materials and Methods

Lipopolysaccharide Extraction and Purification. LPS from *P. aeruginosa* PAO1 (serotype 05) was isolated using the protocol described by Darveau and Hancock.[21] Cultures were grown to an early stationary phase in trypticase soy broth (BBL; 37 °C, 125 rpm), harvested by centrifugation (10 000*g*, 20 min), and washed twice with 0.9% NaCl (w/v). Cells were lyophilized and 1 g (dry weight) of material was extracted. After ultracentrifugation, used to obtain the extracted LPS, samples were dialyzed five times against 5 mM Na_2EDTA (5 mM HEPES, pH 8.0), twice against 50 mM NaCl (5 mM HEPES, pH 8.0), and twice against Nanopure water. Each dialysis step was done for 8 h with continuous stirring and a minimum ratio of 50:1 volume. The dialyzed LPS was then freeze-dried. The LPS was assessed for KDO and LPS banding pattern, as well as DNA and protein contamination and the values obtained were found to be in agreement with the published data.[21]

Preparation of the Oriented Multibilayer Lamellar Samples. Silicon (Si) wafers were cleaned with chloroform in an ultrasonic cleaner and rinsed thoroughly with methanol. Oriented multibilayer samples were prepared by depositing LPS suspended in water on a clean Si substrate. The samples were kept at 45 °C, allowing for the water to evaporate and enabling the self-assembled lipid bilayers to align with respect to the Si substrate (Figure 1). To further improve bilayer orientation, samples were temperature cycled between 8 and 55 °C, while hydrated.

Structure of Lipopolysaccharide Bilayers

J. Phys. Chem. B, Vol. 111, No. 10, 2007 **2479**

Neutron Diffraction Measurements. Neutron diffraction experiments were conducted using the N5 beam line located at the National Research Universal reactor (Chalk River Laboratories, Canada). Neutrons with a wavelength (λ) of 2.37 Å were selected using the (002) reflections of a pyrolytic−graphite (PG) monochromator, while a PG filter was used to eliminate the higher-order reflections (i.e., $\lambda/2$, $\lambda/3$, etc.). For diffraction experiments, samples of aligned LPS on Si substrates were taken in airtight aluminum canisters.[22] The relative humidity (RH) was maintained by placing the appropriate saturated salt solution [e.g., $NaNO_2$ (66%), KCl (84%), and K_2SO_4 (98%)] inside the sample cell. Temperature was controlled to an accuracy of ±0.2 °C using a circulating water bath. Diffraction measurements were performed on two similarly prepared substrates to check for reproducibility of the data, and certain Bragg peaks were remeasured to confirm that the samples were stable over the period that data were collected. The lamellar repeat spacings (*d*-spacings) remained static within the time period of the experiment, and the measured intensities, for a given diffraction peak, remained virtually unaltered (within 10%) during the course of a given experiment.

Neutron Data Analysis. The scattering vector (q) is defined as $q = 4\pi \sin(\phi/2)/\lambda$, where λ is the wavelength and ϕ is the scattering angle. The background over the entire range of the scattering vector (q) was fitted to a second-order polynomial equation, while Bragg peak positions were determined by fitting the Bragg maxima to a Gaussian. *d*-Spacings for the various RH samples were calculated using $n\lambda = 2\pi \sin(\phi/2)$, commonly known as Bragg's law, where n is the order number of the Bragg peak. While the positions of Bragg peaks are a direct measure of *d*-spacing, the peak intensities contain the structural information regarding the bilayers. The Bragg peak intensity, $I(q)$, was determined by integrating the peak area over the scattering vector (q). $I(q)$ was then corrected using the appropriate correction terms, which include the incident flux on the sample (C_{flux}), sample absorption (C_{abs}), and the Lorentz factor (C_{Lor}).[22] The amplitude of the structure factor for each Bragg peak is thus given by $|F(q)|^2 = C_{flux}C_{Lor}C_{abs}I$. SLD profiles, $\rho(z)$, were constructed using the equation, $\rho = \sum_{n=1}^{n=6} F(q)_n \cos(2\pi nz/d)$, where z is the distance along the bilayer normal.

In order to determine the structure factors, it was necessary to perform H_2O/D_2O contrast variation experiments.[23] These experiments were conducted by equilibrating the oriented bilayers at 84% RH at the desired H_2O/D_2O ratio. This method is based on the fact that $|F(q)|$ varies linearly with the water's isotopic composition,[23] and measurements with at least three different isotopic compositions were performed (e.g., Figure 3). Note, that at 8 mol % D_2O we take advantage of the fact that water has a net zero SLD; therefore, practically all of the scattering can be attributed to LPS bilayers, only. Since we chose our origin to be at the center of the bilayer, the greatest contribution by the water takes place at $d/2$. What this means is that when H_2O is replaced by D_2O, the even-order Bragg maxima will increase algebraically, while the inverse holds true for the odd-order structure factors. Thus, the linear plots of structure factor amplitudes versus mol % D_2O should have positive slopes for the even orders and negative slopes for the odd orders.[24] As shown in Figure 3, this behavior is fulfilled for both temperatures. As there is little doubt for our choice of phases for 35 °C LPS bilayers, the consistency between the bilayer profiles at the two different temperatures lends additional justification for our choice of phases concerning the bilayers at 51 °C—this assuming that the bilayers are not drastically
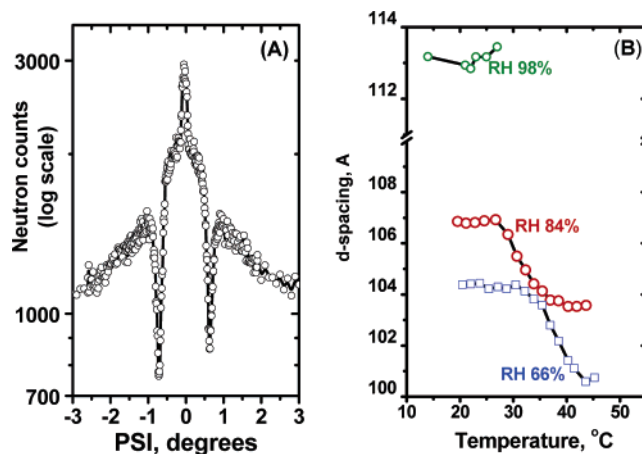

Figure 2. (A) Typical rocking curve of the first-order Bragg maximum from aligned LPS multibilayers. The full width at half-maximum (fwhm) is a good indicator of the sample's orientation with respect to the Si substrate. The minima along the scattering curve are the result of increased neutron absorption, which occurs when the specimen is rotated (PSI) so that either the incident beam or the diffracted beam is parallel to the silicon substrate. (B) Temperature dependence of the lamellar repeat spacing at 66, 84, and 98% relative humidity (RH). At 66 and 84% RH, the transition from the gel to the liquid-crystalline phase is continuous, reflecting the heterogeneous chemistry of LPS molecules. At 98% RH, however, increasing the temperature to 28 °C causes the disappearance of lamellar peaks. See text for details.
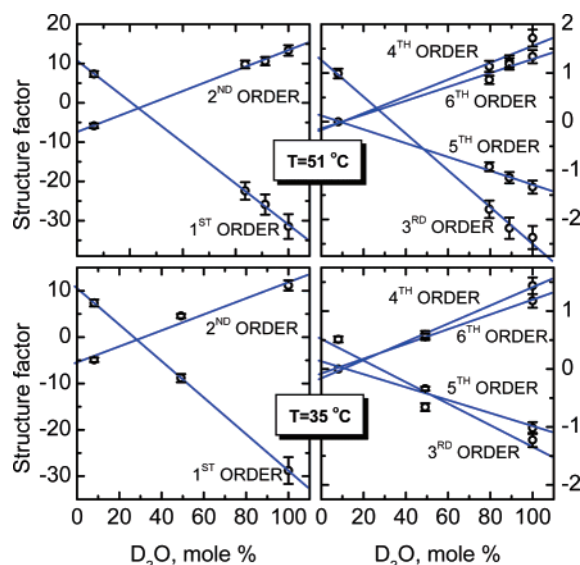

Figure 3. Structure factors, $F(q)$, with 10% error bars for 84% RH LPS bilayers at 51 °C (top panels) and 35 °C (bottom panels) as a function of H_2O/D_2O ratio. As expected, each data set is well fit by a straight line using a least-squares fit.

different from each other, as their *d*-spacings are within a couple of angstroms of each other.

Results and Discussion

Rocking Curve and the Orientation of the LPS Multibilayers. LPS molecules isolated by the Darveau and Hancock method[21] contain a mixture of rough (R) and smooth (S) A-band and B-band LPS, similar to the natural LPS distribution in strain PAO1. At the hydration and temperature regimes investigated, this particular LPS formed highly aligned, multibilayer stacks, as determined from the rocking curve of the first-order Bragg peak (Figure 2A). Note that the width of the rocking curve is

inversely proportional to the degree of bilayer orientation with respect to the Si substrate, while the minima are the result of increased neutron absorption which occurs when the specimen is rotated so that either the incident beam or the diffracted beam is parallel to the Si substrate.

Temperature Scans and Phase Transitions. First- and second-order lamellar reflections were recorded at 84% RH (D$_2$O) at temperatures ranging from ~20 to 45 °C. The temperature dependence of the *d*-spacing is shown in Figure 2B. The *d*-spacing appeared to change at ~30 °C and decreased gradually with increasing temperature from 107 to 103 Å. No further change to the *d*-spacing is observed beyond 40 °C. The change in *d*-spacing can be attributed to the melting transition of the LPS's fatty acid chains. The transition appears to take place over a 10 °C range in temperature (i.e., 30−40 °C), consistent with information in the literature[25,26] and also in agreement with published data for the sodium salt form; changing the salt from a monovalent to a divalent cation has been shown to increase the temperature range significantly.[1] The transition from gel to liquid-crystalline bilayers appears to be continuous, and not as abrupt as commonly observed in single-component phospholipid systems. This can be ascribed to the structural heterogeneity of *P. aeruginosa* LPS. As mentioned previously, this LPS contains five to six variable chain length fatty acid acyl chains and the O-side chains contain a variable number of repeating saccharide units. Lowering the RH to 66% reduces the *d*-spacings of gel and liquid-crystalline bilayers as well as those in the continuous transition region, at the same time shifting their temperatures to higher values. For 66% RH, the transition from gel to liquid crystalline takes place over 10 °C, from 34 to 44 °C, with the gel phase found at higher temperature.

Increasing the RH to 98% resulted in the *d*-spacing increasing to 113 Å (Figure 2B). However, increasing the temperature to 28 °C appeared to destabilize the bilayer structure, causing the lamellar Bragg peaks to practically disappear, suggesting the complete dissolution of a lamellar morphology with long-range order. However, this long-range periodicity is recovered by reducing the temperature to 16 °C, implying that at this particular humidity (98% RH) the bilayers undergo a discontinuous[27] but not a complete unbinding transition, as previously reported in charged phospholipid systems.[28] Diffraction experiments were also performed using fully hydrated LPS bilayers whereby multibilayer stacks of LPS were squeezed between the Si substrate and a glass slide. In this fully hydrated state, the bilayers exhibited similar features (i.e., no Bragg reflections) to those at 98% RH, suggesting that the two conditions produce similar structures. In general, the temperature scan measurements demonstrate that the LPS morphology and its corresponding transition temperatures are influenced by the level of hydration.

Scattering Length Density Profile and the Internal Structure of the LPS Bilayers. Higher-order Bragg peaks were measured at 84% RH (100% D$_2$O) and at two different temperatures, one deep in the L$_\alpha$ phase (51 °C) and the other in the middle of the continuous transition region (35 °C). Bragg peaks occurring up to the sixth-order maximum are observed, indicative of a lamellar morphology with a high degree of long-range order (Figure 4).

Figure 5 shows 1D SLD profiles constructed for both L$_\alpha$ (51 °C) and continuous transition (35 °C) bilayers using structure factors determined by varying the H$_2$O/D$_2$O ratio (Tables 1 and 2). For each profile, the center of the bilayer was placed at the origin. The bilayer is formed by two LPS monolayers with their hydrophilic groups residing in the major water region and the hydrophobic acyl chains of the two monolayers facing each other in the middle.

Knowing the general chemical structure of LPS, we are in a position to rationalize the various features contained in the SLD profiles. The 8.0 mol % D$_2$O SLD profile depicts scattering arising predominantly from the LPS bilayer. This profile should not be confused with 1D SLD profiles of model systems which do not possess the outer core and the complex network of O-side chains present in LPS. As mentioned, the O-side chains are highly variable, both in composition and in length, and they, along with the core, contribute significantly to the thickness of the LPS bilayer (~70 Å compared to ~35 Å for the L$_\alpha$ phosphatidylcholine bilayer).[24] The trough at the center of the SLD profile (i.e., 0 Å) can be attributed to the disordered portion of the acyl hydrocarbon chains and is a characteristic element seen in the SLD of saturated hydrocarbon amphiphiles.[24] The SLD increased steadily from the bilayer center and reached a maximum at ~11 Å. This distance of 11 Å corresponds to those hydrocarbon chains oriented approximately perpendicular to the plane of the bilayer, and is roughly equal to the calculated thickness of the LPS hydrocarbon region (12.5 Å). Note that the LPS acyl chains contain 10−12 carbon atoms; thus, the length of the hydrocarbon chain is ~12.5 Å (10 × 1.25 Å). The SLD region from ~11 to 24 Å corresponds to the lipid A head group and inner core region, which contains chemical groups such as phosphates and carboxylates, and when compared to fatty acid chains have higher SLD values. Specifically, the peak at ~11 Å presumably corresponds to the phosphate group present in the lipid A head region, while the peak at ~24 Å corresponds to the combined phosphate and carboxylate groups present in the core region. The steady reduction in SLD beyond the 24 Å region reflects the significant amount of H$_2$O molecules bound to the chemical residues in the outer core and O-side chain regions, and the relatively lower mass density of chemical residues present in the O-side chains. The SLD behavior, as rationalized in a previous section, verifies that the structure factors were assigned the appropriate phases. This issue was carefully scrutinized, especially the second-order structure factor of the 8 mol % D$_2$O contrast condition at 51 °C, for which the choice of sign can be debated. It should be pointed out, however, that plausible and consistent bilayer profiles at both 51 and 35 °C are only obtained when reconstructing the 1D profiles using the structure factors shown in Table 1.

At 8 mol % D$_2$O, the so-called "null scattering" case, water is effectively invisible to neutrons and any contribution to the SLD can be attributed to the LPS bilayer itself (Figure 5). With increasing D$_2$O content, there is a profound but expected increase in the outer region of the LPS bilayer, as water interacts with the outer core and O-side chains. However, and in contrast to pure phosphatidylcholine bilayers, it is evident that besides wetting the hydrophilic moieties of LPS, water penetrates deep into the bilayer's hydrophobic core, up to and including the terminal methyl groups. Although the changes to the SLD, as a function of D$_2$O content, are subtle, it is quite evident that water is present in the disordered terminal methyl groups, as shown by the increased SLD corresponding to the bilayer's center. Although with the present data we are unable to provide a quantitative description of water distribution along the bilayer, as we do not accurately know the contents of the unit cell and thus cannot calculate the bilayer's average SLD, we can deduce the distribution of water molecules from the difference profiles obtained by subtracting the relative SLD profiles. This subtraction
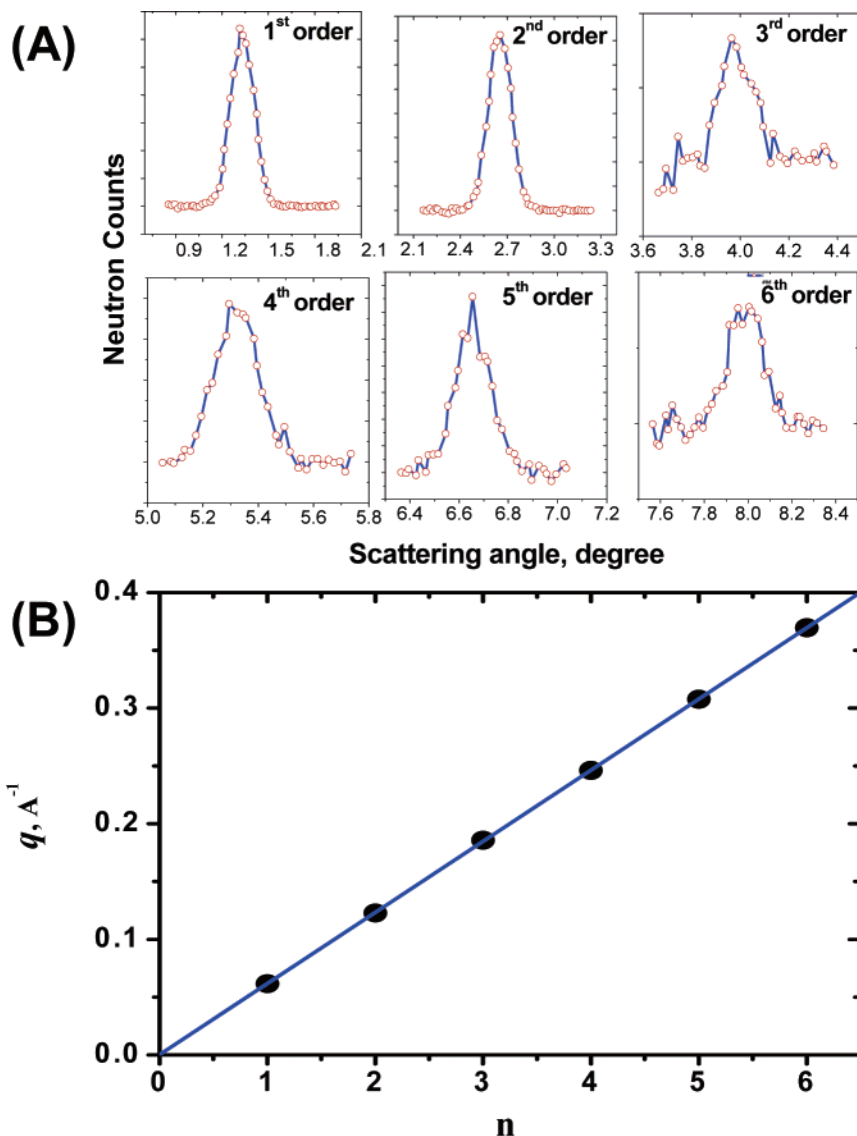
Structure of Lipopolysaccharide Bilayers

J. Phys. Chem. B, Vol. 111, No. 10, 2007 **2481**

Figure 4. (A) Bragg peaks obtained at 84% RH (D_2O) and 51 °C. Up to six orders of Bragg reflections were recorded. Note that longer neutron counting periods have been used to obtain higher-order Bragg peaks. (B) Plot of scattering vector (q) versus order of Bragg peak (n). The diffraction peaks are indicative of bilayers with no trace of non-lamellar phases.

results in the water distribution, on a relative SLD scale, which we define as

$$kP_W(z) - k = \frac{(\rho'_A(z) - \rho'_A(d/2)) - (\rho'_B(z) - \rho'_B(d/2))}{\rho_{WA} - \rho_{WB}}$$

where ρ_{WA} is the SLD of water at a contrast condition A and $\rho'_A(d/2)$ is the relative SLD at a value z, which is equal to half of the d-spacing and where we assume the bilayer contribution to the SLD to be zero (i.e., only water contributes to the SLD). $P_W(z)$ is the distribution of water molecules on an absolute scale, which is further scaled and shifted by the unknown factor k. Subtracting the various SLD profiles (i.e., different contrast conditions) results in six difference profiles at 51 °C and three difference profiles at 35 °C (Figure 6). By comparing these difference profiles, an estimate of the bilayer SLD "standard deviation" is obtained. For the case where two contrast conditions are similar, for example, 100 and 89% D_2O contrast, the subtraction is very sensitive to errors in the SLD of water, the result being an increase in the difference SLD profile uncertainty (shaded regions in Figure 6). This is especially

pronounced in the case of LPS bilayers at 51 °C. Despite this, all of the difference profiles show similar trends for both temperatures and changing any of the phases results in much larger uncertainties (data not shown). In summary, even though we cannot quantitatively describe the distribution of water along the bilayer, its presence in the bilayer is irrefutable. Moreover, this penetration of water is similar for both L_α and continuous transition LPS bilayers (see Figures 5 and 6).

So how can one reconcile this unexpected outcome which contradicts traditional lipid bilayer hydration dogma? First, this LPS is clearly polyanionic with the anionic groups residing predominantly in the lipid A head group (monophosphate) and oligosaccharide core region (e.g., carboxyl groups of KDO residues). Considering that lipid A usually contains five to six hydrocarbon acyl chains, the density of formal negative charges is more than 1 per hydrocarbon chain, twice that of common acidic phospholipids. This elevated charge density may have the effect of reducing the lateral interactions between LPS molecules, allowing easier access of water into the bilayer. Second, this LPS system is in the sodium (Na) salt form (see the Materials and Method section for details). Opportunistic
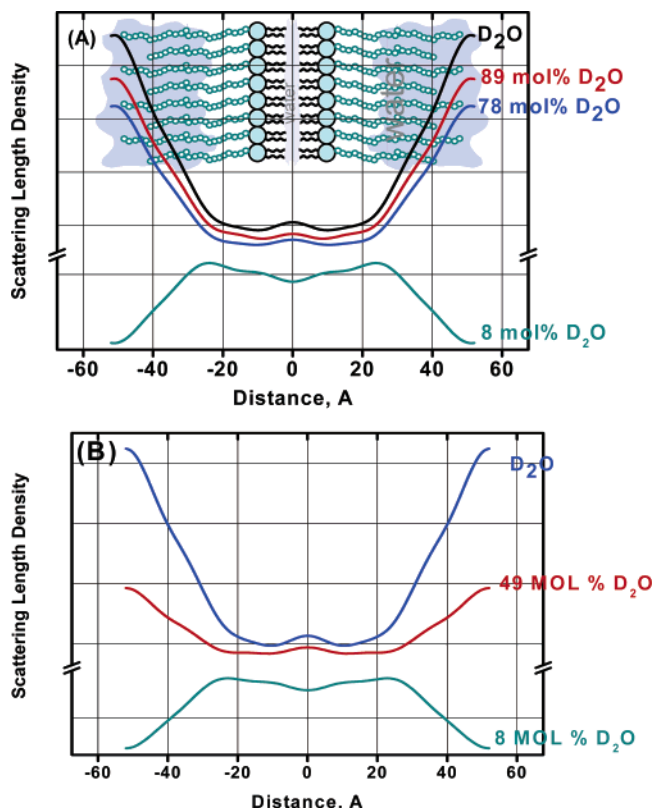
Figure 5. (A) Scattering length density profiles of liquid-crystalline LPS bilayers at 84% RH and 51 °C. The 1D SLD profiles for all D_2O compositions, namely, 100, 89, 78, and 8 mol % D_2O, are shown. For each profile, the center of the bilayer was placed at the origin. The bilayer is formed by two LPS monolayers with their hydrophilic groups on the outside and the hydrophobic chains of the two monolayers apposing each other (center of bilayer). For clarity, the profiles have been shifted with respect to each other. D_2O seems to penetrate the entire length of the bilayer. (B) SLD profiles of LPS bilayers at 84% RH and 35 °C. The structural features are similar to those observed for bilayers at 84% RH and 51 °C.

TABLE 1: Structure Factors of LPS Bilayers at 51 °C and 84% RH

% D_2O content	Bragg reflection					
	1	2	3	4	5	6
100%	−31.48	13.36	−2.371	1.718	−1.336	1.337
89%	−25.89	10.61	−2.180	1.239	−1.144	1.187
79.5%	−22.42	9.810	−1.792	1.137	−0.9190	0.8609
8%	7.349	−5.842	0.9907	0	0	0

TABLE 2: Structure Factors of LPS Bilayers at 35 °C and 84% RH

% D_2O content	Bragg reflection					
	1	2	3	4	5	6
100%	−28.80	11.15	−1.226	1.437	−1.018	1.177
49.2%	−8.824	4.567	−0.6586	0.5541	−0.3388	0.5960
8.1%	7.378	−4.892	0.5119	0	0	0

pathogens such as *P. aeruginosa* and coliforms (e.g., *Escherichia coli*, *Salmonella*, and *Shigella*) are subjected to high Na^+ concentrations in serum while infecting tissue. Our experiments have been done with Na^+ as the predominant cation. As such, this form of LPS should be a better mimic of disease than the multivalent salt forms of the lipid. In agreement with previously published data for both monovalent and divalent cations, Na^+ seems to have a profound effect on water permeability, as the
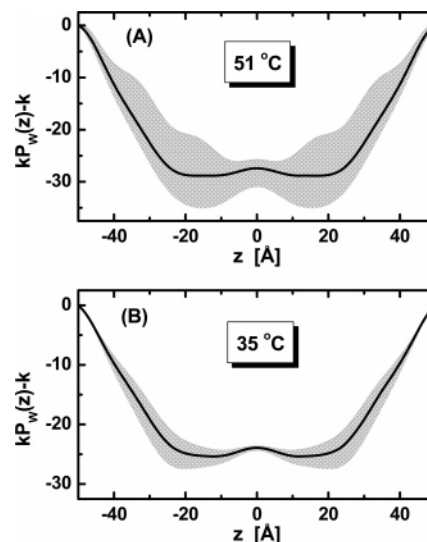

Figure 6. Distribution of water along 51 °C (A) and 35 °C (B) LPS bilayers. The width of the shaded areas indicates the uncertainty in determining the distribution of water. The larger uncertainty shown for the 51 °C water distribution, compared with the 35 °C distribution, is the result of subtracting similar contrast condition SLD (e.g., 100 and 89% D_2O). Ideally, for a given temperature, a single curve should describe this distribution.

salt bridging between LPS molecules is affected.[1,3,16] Regardless of the actual mechanism that enables water to penetrate, the data clearly show that water permeates the entire length of the LPS bilayer including the bilayer center and this has implications for the penetration of small molecules into and across the OM. This result seems to apply equally to L_α and continuous transition bilayers.

Finally, it is known that fully hydrated suspensions of LPS can adopt a number of morphologies including non-lamellar structures.[17,18] As was discussed, 98% RH bilayers destabilize at 28 °C (i.e., lamellar Bragg reflections disappear), while fully hydrated LPS does not even form bilayers. Now that we know that LPS bilayers are permeable to water, it therefore seems that the formation of bilayers is highly dependent on the amount of water present in the hydrophobic core, and any excess results in the multibilayers breaking up.

Concluding Remarks

The lipid packing order of phospholipid bilayers can frequently be affected by external ions so that the polar head groups capture metal cations, thereby becoming a particular salt form. In this respect, LPS bilayers are no different from those bilayers formed by phospholipids. LPS in the outer membrane of Gram-negative bacteria is also affected by metal cations, Mg^{2+} and Ca^{2+} being preferred since they salt-bridge adjacent LPS molecules together.[29] This adds stability to the outer membrane and may limit water permeability. As shown by neutron scattering, the permeability of LPS bilayers is altered in the presence of a monovalent cation, namely, Na^+. Neutron experiments are now being planned to study other LPS salt forms and their permeability to water.

Structure of Lipopolysaccharide Bilayers

J. Phys. Chem. B, Vol. 111, No. 10, 2007 **2483**

References and Notes

(1) Nikaido, H. *Microbiol. Mol. Biol. Rev.* **2003**, *67*, 593.

(2) Rocchetta, H. L.; Burrows, L. L.; Lam, J. S. *Microbiol. Mol. Biol. Rev.* **1999**, *63*, 523.

(3) Wilkinson, S. G. *Prog. Lipid Res.* **1996**, *35*, 283.

(4) Kamio, Y.; Nikaido, H. *Biochemistry* **1976**, *15*, 2561.

(5) Smit, J.; Kamio, Y.; Nikaido, H. *J. Bacteriol.* **1975**, *124*, 942.

(6) Hancock, R. E. W.; Nikaido, H. *J. Bacteriol.* **1978**, *136*, 381.

(7) Lam, J. S.; Matewish, M.; Poon, K. K. H. In *Pseudomonas, Volume 3—Biosynthesis of Macromolecules and Molecular Metabolism*; Ramos, J.-L., Ed.; Kluwer Academic/Plenum Publishers: New York, 2004; p 3.

(8) Ernst, R. K.; Yi, E. C.; Guo, L.; Lim, K. B.; Burns, J. L.; Hackett, M.; Miller, S. I. *Science* **1999**, *286*, 1561.

(9) Sadovskaya, I.; Brisson, J. R.; Lam, J. S.; Richards, J. C.; Altman, E. *Eur. J. Biochem.* **1998**, *255*, 673.

(10) Sadovskaya, I.; Brisson, J. R.; Thibault, P.; Richards, J. C.; Lam, J. S.; Altman, E. *Eur. J. Biochem.* **2000**, *267*, 1640.

(11) Vaara, M. *Microbiol. Rev.* **1992**, *56*, 395.

(12) Labischinski, H.; Barnickel, G.; Bradaczek, H.; Naumann, D.; Rietschel, E. T.; Giesbrecht, P. *J. Bacteriol.* **1985**, *162*, 9.

(13) Kastowsky, M.; Gutberlet, T.; Bradaczek, H. *Eur. J. Biochem.* **1993**, *217*, 771.

(14) Ding, L.; Yang, L.; Weiss, T. M.; Waring, A. J.; Lehrer, R. I.; Huang, H. W. *Biochemistry* **2003**, *42*, 12251.

(15) Snyder, S.; Dennis, K.; McIntosh, T. J. *Biochemistry* **1999**, *38*, 10758.

(16) Garidel, P.; Rappolt, M.; Schromm, A. B.; Howe, J.; Lohner, K.; Andra, J.; Koch, M. H.; Brandenburg, K. *Biochim. Biophys. Acta* **2005**, *1715*, 122.

(17) Naumann, D.; Schultz, C.; Sabisch, A.; Kastowsky, M.; Labischinski, H. *J. Mol. Struct.* **1989**, *214*, 213.

(18) Seydel, U.; Koch, M. H.; Brandenburg, K. *J. Struct. Biol.* **1993**, *110*, 232−243.

(19) Katsaras, J. *Biochem. Cell Biol.* **1995**, *73*, 209 and references therein.

(20) Katsaras, J.; Raghunathan, V. A. In *Lipid Bilayers: Structure and Interactions*; Katsaras, J., Gutberlet, T., Eds.; Springer: Berlin, 2001; p 25.

(21) Darveau, R. P.; Hancock, R. E. W. *J. Bacteriol.* **1983**, *155*, 831.

(22) Harroun, T. A.; Katsaras, J.; Wassall, S. R. *Biochemistry* **2006**, *45*, 1227.

(23) Worcester, D. L.; Franks, N. P. *J. Mol. Biol.* **1976**, *100*, 359.

(24) Franks, N. P.; Lieb, W. R. *J. Mol. Biol.* **1979**, *133*, 469−500.

(25) Brandenburg, K., Andra, J., Muller, M., Koch, M. H. J., Garidel, P. *Carbohydr. Res.* **2003**, *338*, 2477.

(26) Tong, J.; McIntosh, T. J. *Biophys. J.* **2004**, *86*, 3759.

(27) Pozo-Navas, B.; Raghunathan, V. A.; Katsaras, J.; Rappolt, M.; Lohner, K.; Pabst, G. *Phys. Rev. Lett.* **2003**, *91*, 028101-1.

(28) Nieh, M.-P.; Raghunathan, V. A.; Kline, S. R.; Harroun, T. A.; Huang, C.-Y.; Pencer, J.; Katsaras, J. *Langmuir* **2005**, *21*, 6656.

(29) Ferris, F. G., Beveridge, T. J. *Can. J. Microbiol.* **1986**, *32*, 594.